Proteomic analysis reveals zinc-finger CCHC-type containing protein 3 as a factor inhibiting virus infection by promoting innate signaling

Xiaoyong Chen [a,b,*], Ziwei Li [a], Shuaiwei Wang [a], Guangzhi Tong [b], Keyuan Chen [c], Yan Zhao [a,*]

[a] Department of Livestock and Poultry Infectious Diseases, Institute of Animal Sciences, Wenzhou Academy of Agricultural Sciences, Zhejiang, People's Republic of China
[b] Shanghai Veterinary Research Institute, Chinese Academy of Agricultural Sciences, Shanghai, People's Republic of China
[c] Union Hospital, Fujian Medical University, Fuzhou, People's Republic of China

ARTICLE INFO

ABSTRACT

Influenza a virus exploits host machinery to benefit its replication in host cells. Knowledge of host factors reveals the complicated interaction and provides potential targets for antiviral treatment. Here, instead of the traditional proteomic analysis, we employed a 4D label free proteomic method to identify cellular factors in A549 cells treated with avian H9N2 virus. We observed that 425 proteins were upregulated and 502 proteins were downregulated. Western blotting and quantitative real-time PCR results showed that the zinc-finger CCHC-type containing protein 3 (ZCCHC3) levels were markedly induced by H9N2 infection. Transient expression assay showed that ZCCHC3 expression decreased NP protein levels and viral titers, whereas knockdown of ZCCHC3 enhanced viral growth. Specifically, ZCCHC3 promoted the expression of IFN-β, leading to the increased transcription of IFN downstream antiviral factors. Surprisingly, viral NS1 protein was able to antagonize the antiviral effect of ZCCHC3 by downregulating IFN-β. Eventually, we observed that chicken finger CCCH-type containing protein 3, named ZC3H3, could also suppress the replication of H9N2 virus and the coronavirus-infectious bronchitis virus (IBV) in DF-1 cells. Together, our results showed the cellular proteomic response to H9N2 infection and identified ZCCHC3 as a novel antiviral factor against H9N2 infection, contributing to the understanding of host-virus interaction.

1. Introduction

Influenza virus belongs to the Orthomyxovirus family, with a negative-sense single-stranded RNA genome, which consists of eight segmented negative-stranded RNA (PA, PB1, PB2, HA, NA, NP, NS, and M), encoding more than 17 proteins (Bouvier and Palese, 2008; Chen et al., 2018). It can be classified into four genera, including A, B, C, and D, of which influenza a virus (IAV) is the most detrimental, infecting a wide range of species, including humans, birds, dogs, and pigs (Long et al., 2019). Based on the genetic and antigenic variability of surface glycoproteins, IAV can be further categorized into 18 subtypes of hemagglutinin (HA) and 11 subtypes of neuraminidase (NA) (Tong et al., 2013; Wu et al., 2014). IAV could give rise to seasonal epidemics, and even global outbreaks due to the antigenic shift or drift. The most known is the 1918 Spanish flu, and the recent 2009 H1N1 pandemic, both of which were H1N1 serotype and resulted in severer illness than seasonal epidemics (Sullivan et al., 2010; Trilla et al., 2008). Of note, avian influenza viruses (AIVs), such as H5N1 and H7N9, were threating

human population (Guan and Smith, 2013; Wu et al., 2020). Although AIV infection is limited from person to person, it is worth noting that accumulated mutations of AIVs could facilitate their spread and thus may cause a serious outbreak.

AIVs are one of the contagious agents responsible for respiratory tract symptoms in animals and humans. They are classified into highly pathogenic avian influenza virus (HPAIV) and low pathogenic avian influenza virus (LPAIV). LPAIV infection contributes to mild respiratory disturbance and decreased egg production, while HPAIV infection leads to a marked increase in mortality in chickens (Bui et al., 2018). Additionally, the H5 and H7 subtypes of AIVs, that pose a risk to public health, should be a concern, as evidenced by hundreds of human cases caused by H5N1 and H7N9 viruses (Poovorawan et al., 2013). Of note, H9N2 virus, which has been considered as the most epidemic AIV type, can mutate into HPAIV (Gu et al., 2017). In spite of numerous works done, the host factors that regulate influenza virus infection, especially the H9N2 infection, are not fully addressed. Therefore, it is necessary to investigate host factors acting on influenza virus infection, which can

further promote the understanding of cell-virus interactions.

Upon IAV infection, host pathogen recognition receptors (PRRs) immediately detect the viral components-pathogen associated molecular patterns (PAMPs), which results in the activation of innate signaling, inducing the expression of numerous antiviral genes (Chen et al., 2021). Previous studies have demonstrated that zinc finger proteins (ZFPs) play an important role in modulating innate signaling against virus infection. For example, zinc finger CCCH-type antiviral protein 1 (ZC3HAV1), identified as an interferon-stimulated gene (ISG), inhibits A/WSN/33 virus (H1N1) and Sendai virus (SeV) infections by potentiating the interferon (IFN) signaling (Zhang et al., 2020). Monocyte chemoattractant protein 1-induced protein 1 (MCPIP1), also known as ZC3H12A, is an antiviral protein against a wide range of viruses, including dengue virus (DENV), hepatitis C virus (HCV), and Japanese encephalitis virus (JEV), through targeting and degrading viral RNA in a nuclease-dependent manner (Lin et al., 2013).

Interestingly, zinc finger C3H1 domain-containing protein (ZFC3H1) suppresses human immunodeficiency virus (HIV) infection through a distinct mechanism by which ZFC3H1 inhibits long term repeat (LTR)-directed transcription (Contreras et al., 2018). Further, ZFC3H1 could serve as a biomaker for the diagnosis of prostate adenocarcinoma (PRAD), which significantly promotes the development of new treatments to treat PRAD (Huang et al., 2021). Recently, a novel member, zinc-finger CCHC-type containing protein 3 (ZCCHC3), was identified to interact with retinoic acid-inducible gene I (RIG-I) and cyclic GMP-AMP synthase (cGAS) to strengthen innate immune response to RNA and DNA virus infections (Lian et al., 2018a, 2018b). Whether ZCCHC3 serves as a regulator in influenza virus infection remains still unknown.

In this study, we employed a 4D label free proteomic method to identify host factors that could regulate H9N2 virus infection. We found that ZCCHC3 was markedly induced and investigated its effects and the underlying mechanisms on H9N2 infection. The overexpression and knockdown assays showed that ZCCHC3 had an antiviral activity on H9N2 infection. Furthermore, upregulation of ZCCHC3 resulted in increased expression of cytokines and ISGs. Interestingly, viral NS1 protein antagonized ZCCHC3-mediated IFN signaling, thus assisting viral replication. These data demonstrated that ZCCHC3 acts as a critical role against H9N2 infection.

2. Materials and methods

2.1. Cells and viruses

A549 cells (CCL-185, ATCC), HEK293T cells (CRL-11, ATCC), and DF-1 cells (CRL-12203, ATCC) were kept in our laboratory. They were cultured in Dulbecco's modified Eagle's medium (DMEM; Invitrogen) supplemented with 10% fetal bovine serum (FBS; Gibco) at 37°C under 5% CO_2. The Lipofectamine 3000 Reagent (L3000015, Invitrogen) was used to transfect cells with the indicated plasmids when cells were grown to approximately 70%-80% confluence, while the Lipofectamine RNAiMAX (13778150, Invitrogen) was used to transfect cells with the siRNA when cells were grown to 50%-60% confluence.

H9N2 virus (AV1551) was provided by the China Veterinary Culture Collection Center (CVCC, Beijing, China). It was amplified using specific pathogen free chicken embryo. The viral titer was determined and exhibited as tissue culture infectious dose 50 ($TCID_{50}$). A549 cells or HEK293T cells were infected with the virus at an MOI of 1, together with 1 µg/ml TPCK-treated trypsin (4370285-1KT, Merck). After incubation at 37°C for 1 h, the unattached viruses were washed and removed by phosphate buffer saline (PBS; Beyotime). Then, the cells were maintained in DMEM supplemented with 10% FBS and collected at the different time points based on the requirements. Infectious bronchitis virus (IBV; AV1533, CVCC) was kept in our laboratory.

2.2. Antibodies, agents, and plasmids

Antibody against ZCCHC3 (30000–1) was obtained from Signalway Antibody. Antibody against UBE2C (12134-1), antibody against PIP5K1A (15713-1), antibody against β-actin/ACTB (66009-1), HRP-conjugated antibody against mouse IgG (SA00001-1), and HRP-conjugated antibody against rabbit IgG (SA00001-2) were purchased from the Proteintech Group. Antibody against DHCR24 (PTM-6171) and antibody against P4HA2 (PTM-6033) were obtained from PTM Biolabs (Hangzhou, China). Antibody against nucleoprotein (NP) was prepared in our laboratory. Antibody against Flag (AF5051) was purchased from Beyotime. Antibody against Myc (M4439) was obtained from Sigma-Aldrich.

The pcDNA3.1 (Invitrogen) plasmid was kept in our laboratory. To construct the recombinant plasmids, the target genes were amplified. The PCR products were purified and determined. After digestion, the pcDNA3.1 and purified PCR products were ligated using the ClonExpress II One Step Cloning Kit (C112-02, Vazyme Biotech, Nanjing, China). After sequencing, the recombinant plasmids were stored in -20°C.

2.3. Cell viability assay

To assess the viability of the transfected cells, cells were digested and collected after 36 h transfection. The viability was detected and analyzed using Trypan Blue Staining Cell Viability Assay Kit (C0011, Beyotime), according to the instructions.

2.4. Western blotting and quantitative real-time PCR

After washing twice using PBS, cells were lysed in RIPA Lysis Buffer (P0013B, Beyotime) including protease and phosphatase inhibitor cocktail. The lysates were then eluted in SDS loading buffer. After denaturation, the lysates were separated with SDS-PAGE. The proteins were then transferred to nitrocellulose membranes (10600001, GE Healthcare). After that, the membranes were blocked using Quick-Block™ Blocking Buffer (P0252, Beyotime) for 15 min at room temperature. Next, the membranes were interacting with the primary antibody at room temperature for 2 h. After washing for 30 min using TBS, the membranes were bound with the secondary antibody. After washing, the proteins were detected using enhanced chemiluminescence (ECL; P0018FS, Beyotime). The ImageJ software (NIH, USA) was used to analyze the target protein bands.

Total RNA extraction was performed using RNAsimple Kit (DP419, TIANGEN) according to the protocols. The RNA was reverse-transcribed using PrimeScript RT Master Mix (Takara, Japan). Quantitative real-time PCR analysis was performed using

BeyoFast™ SYBR Green qPCR Mix (2X) (D7260, Beyotime) with cDNA and primers. Primer sequences were shown in Table S1 and Table S2 as previously reported (Lian et al., 2018b; Zhang et al., 2020). The RNA levels of samples were analyzed using LightCycler*R*96 system (Roche, Switzerland).

2.5. Elisa

The secretion of human IFN-β was calculated using Human IFN-β Elisa Kit (SEKH-0410, Solarbio), according to the instructions. The culture supernatant was collected and injected to microELISA strip plate wells. After binding with the specific antibody, the samples were incubated to interact with the horseradish peroxidase-conjugated antibody. After washing, the samples in each well were injected to the tetramethylbenzidine (TMB) substrate solution. Then, the content was measured through the optical density (OD) spectrophotometrically at 450 nm when the stop solution was added. Finally, the secretion of IFN-β in these samples was analyzed by calculating the OD of the samples and the standard curve.

2.6. Sample preparation

The A549 cells were collected from two groups at 24 hours post infection (hpi), namely the H9N2 group and the mock group, with three replicates in each group. The samples were then sent to PTM Biolab under dry ice. Briefly, cells were sonicated three times on ice using a high intensity ultrasonic processor (Scientz) in lysis buffer supplemented with protease inhibitor. The debris was removed by centrifugation at 12,000 g at 4°C for 15 min. Then, the supernatant was harvested and the protein concentration was determined using Easy II Protein Quantitative Kit (DQ111-01, TransGen Biotech).

2.7. Mass spectrum analysis

4D label free proteomics is based on the traditional 3D separation of the three dimensions of retention time, mass-to-charge ratio and ion intensity, with an addition of a fourth dimension - the separation of ion mobility, thus significantly improving the scanning speed, detection sensitivity, and the performance of proteomics in terms of identification depth, detection cycle and quantitative accuracy. Briefly, the solvent A (0.1% formic acid, 2% acetonitrile/in water) was used to dissolve the tryptic peptides, which were then loaded onto a home-made reversed-phase analytical column. After that, peptides separation was performed with a gradient from 6% to 24% solvent B (0.1% formic acid in acetonitrile) over 70 min, 24% to 35% in 14 min, and up to 80% in 3 min. Finally, it was holding at 80% for the last 3 min, at a constant flow rate of 450 nL/min on a nanoElute UHPLC system (Bruker Daltonics). These peptides were next analyzed by capillary source and by the timsTOF Pro (Bruker Daltonics) mass spectrometry. Precursors and fragments were analyzed on a TOF detector, with an MS scan range from 100 to 1700 m/z. The timsTOF Pro was performed in parallel accumulation serial fragmentation (PASEF) mode. Precursors with charge states 0 to 5 were selected for fragmentation, and 10 PASEF-MS/MS scans were obtained per cycle. The dynamic exclusion was set to 30 s.

2.8. Bioinformatics analysis

Gene Ontology (GO) annotation was performed according to the UniProt-GOA database. Specifically, identified protein ID was converted to UniProt ID, which was then mapped to GO IDs by protein ID. If the identified proteins were not annotated by UniProt-GOA database, the InterProScan soft would be employed to annotated protein's GO functional based on protein sequence alignment method. A protein domain is a conserved part of a given protein sequence and structure that can evolve, function and exist independently of the rest of the protein chain. According to protein sequence alignment method, the InterProScana and the InterPro domain database were used to annotate the identified protein domains. In addition, Kyoto Encyclopedia of Genes and Genomes (KEGG) database was employed to annotate protein pathways. The KEGG online service tools KAAS was used to annotate protein's KEGG database description and map the annotation result on the KEGG pathway database. Finally, the WoLF PSORT was used to predict subcellular localization.

For GO annotation, a two-tailed Fisher's exact test was used to examine the enrichment of the differentially expressed proteins among all identified proteins. The GO with a corrected p-value < 0.05 is considered significant. For the enrichment of protein domain, InterPro database was researched and a two-tailed Fisher's exact test was employed to investigate the enrichment of the differentially expressed proteins among all identified proteins. Protein domains with a corrected p-value < 0.05 were considered significant. For further hierarchical clustering, all the categories obtained after enrichment along with their values were collated, and then filtered. These categories were enriched in one of the clusters with P value <0.05. All differentially expressed protein database accessions or sequences were searched using the STRING database version 11.0 for protein-protein interactions. The

interactions between the proteins belonging to the searched data set were selected, thereby excluding external candidates. Interaction network form STRING was visualized in R package "networkD3".

2.9. Statistical analysis

Experimental data were exhibited as the means ± standard deviations (SD) based on three independent experiments. Statistical analysis was performed using GraphPad Prism 6.0. The unpaired Student's t test was conducted to compare two groups and one-way analysis of variance (ANOVA) followed by Dunnett's multiple-comparison post hoc test was employed to test differences between the groups. A P value less than 0.05 was used for indicating significance: *, P<0.05; **, P<0.01.

3. Results

*3.1. Cellular proteomic analysis in response to H9N2 virus infection*

We employed a 4D label free proteomic method to identify cellular factors, which could be differentially expressed during H9N2 infection. First, we evaluated the samples and found the samples were qualified to be tested (Fig. S1), as the replicates had good correlation. As a result, a total of 65,914 peptides and 6,308 proteins were identified (Table S3). More specifically, 425 proteins were upregulated while 502 proteins were downregulated (Fig. 1). The subcellular localization analysis (Fig S2) showed that these differentially expressed proteins were located to nucleus (34.74%), cytoplasm (27.4%), extracellular (11.54%), plasma membrane (9.92%), mitochondria (8.95%), nucleus and cytoplasm (4.42%), and others (3.02%). The GO analysis (Fig. 2A) showed these proteins were mainly involved in cellular process, biological process, metabolic process, binding, and catalytic activity. The KEGG analysis was used to show the molecular pathways and cellular processes. As shown in Fig. 2B, these proteins were mainly enriched in glutathione metabolism, cell adhesion molecules, and adherens junction. Further, COG/KOG analysis showed these proteins were enriched in transcription, signal transduction mechanisms, posttranslational modification, protein turnover, and chaperons (Fig. S3).

Next, the biological process analysis showed that these proteins were mainly associated with regulation of defense response, lipid transport, response to transforming growth factor beta, and cholesterol metabolic process (Fig S4). The cellular component analysis displayed that these proteins were involved in plasma membrane and ruffle membrane (Fig S5). Then, we analyzed the molecular function of these proteins and found that they primarily functioned in cell adhesion molecule binding, p53 binding, integrin binding, and monooxygenase activity (Fig S6). Next, we analyzed the protein domain and discovered that the immunoglobin V-set domain, chrome domain, CD80-like C2-set immunoglobulin domain, and iron-binding zinc finger CDGSH type were mainly included (Fig S7). Finally, we performed the PPI network analysis, as it included the direct or indirect interaction between proteins (Fig S8).

The top 20 upregulated proteins were listed in Table 1. The top 20 downregulated proteins were shown in Table 2. Among the upregulated proteins, many of them were involved in innate immunity, including gamma-interferon-inducible protein 16 (IFI16), ISG 15, interferon-induced protein with tetratricopeptide repeats 1 (IFIT1), ZCCHC3, and tumor necrosis factor receptor superfamily member 10A (TNFRSF10A), indicating the activation of innate immunity by H9N2 infection.

3.2. Expression of ZCCHC3 during H9N2 infection

According to the proteomic analysis and previous studies, several factors were selected and validated. NP is selected to show the protein level because NP is the scaffolding protein that supports the viral genome and is involved in the transcription, replication, intracellular transport and packaging of viral RNA. Moreover, NP protein is highly conserved in influenza virus (Watanabe et al., 2010). As shown in
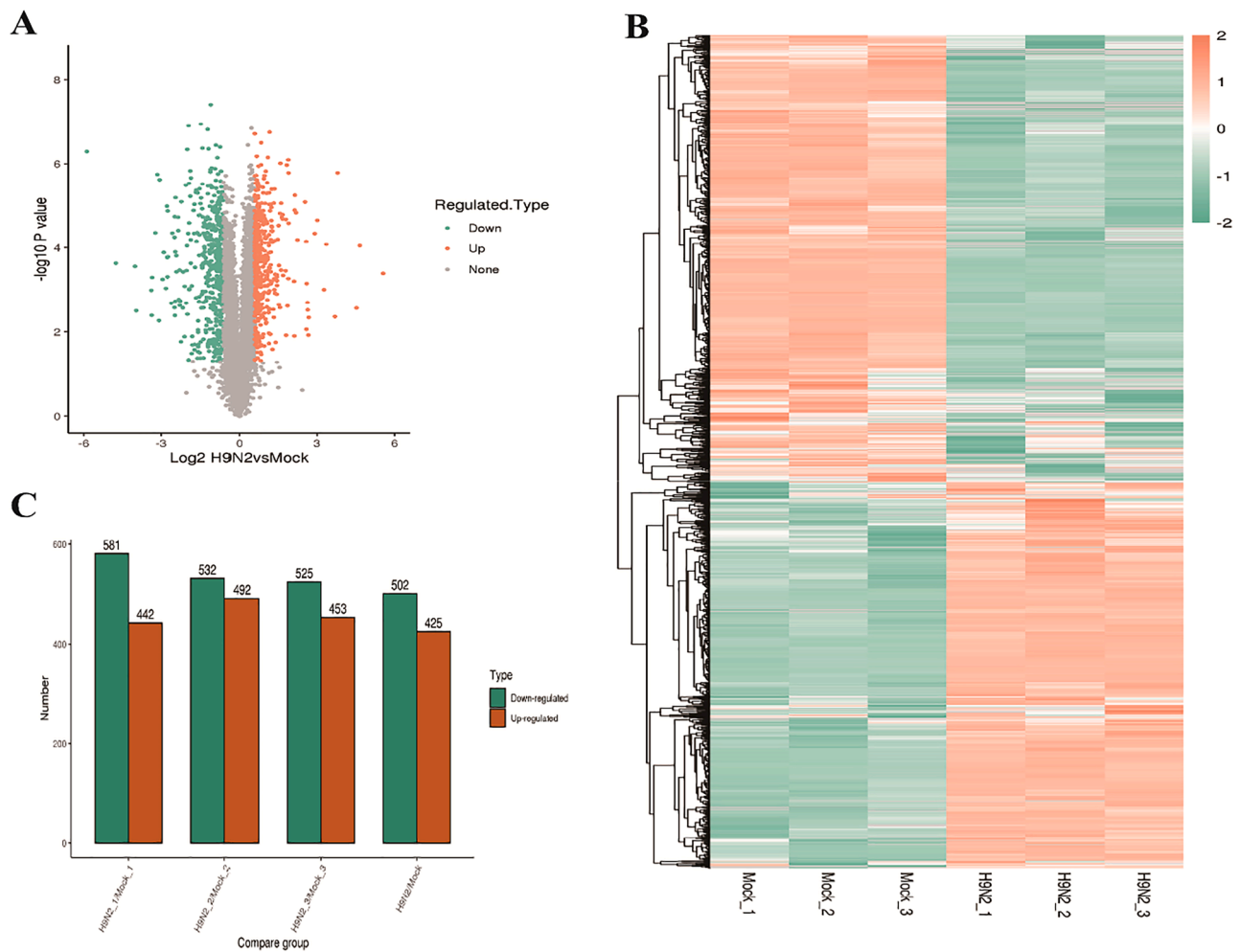
Fig. 1. The differentially expressed proteins in response to viral infection.
(A) Volcano plot. (B) Heat map. (C) Statistical analysis.

Fig. 3A, compared to the mock group, the protein level of ZCCHC3 was enhanced during virus infection. The mRNA level was also enhanced (Fig. 3B). To determine whether the expression of ZCCHC3 was cell-specific, we examined ZCCHC3 in other virus-infected cells. Unfortunately, the antibody against ZCCHC3 did not work well in MDCK cells, DF-1 cells, or Vero cells. Hence, we detected ZCCHC3 in virus-infected HEK293T cells. As a result, the protein level and the mRNA level of ZCCHC3 were also increased (Fig. 3C and D). These data suggested that H9N2 infection could upregulate the endogenous expression of ZCCHC3 in A549 cells and HEK293T cells.

3.3. Expression of other factors in A549 cells during H9N2 infection

To further confirm the results obtained by proteomic analysis, other factors were also examined. As shown in Fig. 4A, the delta (24)-sterol reductase (DHCR24) protein and mRNA levels in virus-infected A549 cells were lower than these in the mock-infected cells. Similarly, the prolyl 4-hydroxylase subunit alpha-2 (P4HA2) levels were also decreased (Fig. 4B). Conversely, we found that the ubiquitin-conjugating enzyme E2 C (UBE2C) and phosphatidylinositol 4-phosphate 5-kinase type-1 alpha (PIP5K1A) levels were enhanced (Fig. 4C and D). These data suggest that the results from proteomic analysis is effective, as confirmed by the experimental results.

3.4. Antiviral effect of ZCCHC3 against H9N2 infection

We showed interest in ZCCHC3, which functions as a zinc finger protein and involves innate immunity. First, we examined whether the plasmids expressing ZCCHC3-Myc were cytotoxic. As shown in Fig. 5A, no significant changes were observed between the groups. Then, we determined its effects on H9N2 infection. We found that the NP protein level was lower in ZCCHC3-overexpressing cells than that in the control cells (Fig. 5B). We also found the virus titer was significantly reduced in ZCCHC3-overexpressing cells (Fig. 5C). To further confirm the effects, siRNA targeting ZCCHC3 was synthesized and transfected into A549 cells. The cell viability showed no significant changes (Fig. 5D). The NP protein levels were enhanced in ZCCHC3-knockdown cells (Fig. 5E). The virus titers were also elevated compared to the control groups (Fig. 5F). Collectively, these data suggest that ZCCHC3 has an antiviral effect on H9N2 infection.

3.5. ZCCHC3 promotes the expression of IFN-β and other antiviral genes

Next, we aimed to uncover the underlying mechanisms by which ZCCHC3 inhibits H9N2 infection. In recent years, accumulating evidence showed that the host factors, including Mx1 and ISG20 could markedly inhibit influenza virus replication through modulating innate immune response (Fatima et al., 2019; Qu et al., 2016). Hence, we investigated whether ZCCHC3 affected innate signaling. We found that ZCCHC3 overexpression could promote the mRNA level of IFN-β

A

B
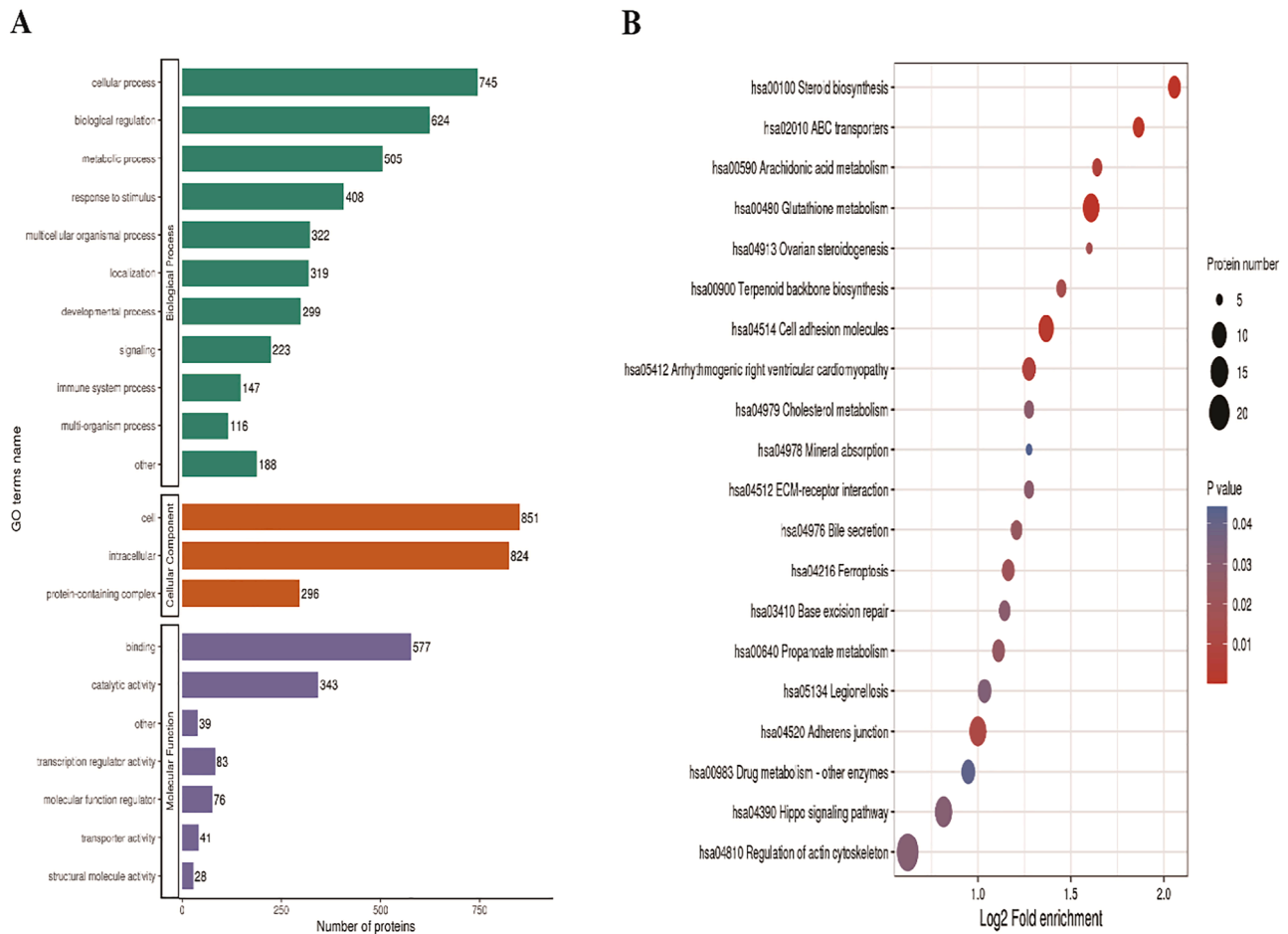
Fig. 2. GO and KEGG enrichment analysis of the differentially expressed proteins. (A) GO analysis. (B) KEGG analysis.

(Fig. 6A). Consistent with this, the secretion of IFN-β were also higher than in the control group (Fig. 6B). Next, we analyzed the expression of IFN downstream antiviral genes. As expected, the mRNA levels of IL-6 and TNF-α were significantly upregulated in A549 cells (Fig. 6C and D). Moreover, the mRNA levels of Mx1 and ISG56, were also upregulated (Fig. 6E and F). These data demonstrated that ZCCHC3 expression leads to upregulation of IFN-β and downstream products, thus suppressing viral growth.

3.6. NS1 protein attenuates the antiviral effect of ZCCHC3

It is well-known that NS1 is a potent inhibitor against innate immunity (Chen et al., 2018). Thus, we hypothesized that NS1 could suppress the antiviral activity of ZCCHC3 on H9N2 infection. As shown in Fig. 7A, the virus titer from cells transfected with ZCCHC3-Myc alone was significantly lower than in the cells transfected with the pcDNA3.1. However, as expected, when the NS1-Flag was added, the virus titer was markedly increased compared to the group expressing ZCCHC3-Myc alone. Moreover, the presence of NS1-Flag downregulated the mRNA level of IFN-β mediated by ZCCHC3 (Fig. 7B). These results suggested that NS1 could antagonize ZCCHC3-mediated IFN-β signaling, thereby aiding in H9N2 replication.

3.7. Chicken zinc finger CCCH-type containing protein 3 (ZC3H3) negatively regulates the growth H9N2 virus and infectious bronchitis virus (IBV)

Similar to IAV, IBV is also an enveloped RNA virus. We then tested

the effect of chicken zinc finger CCCH-type containing protein 3 (ZC3H3) on the growth of H9N2 and IBV. First, ZC3H3 was cloned and expressed (Fig. 8A). The siRNA targeting ZC3H3 was also synthesized (Table S1) and the knockdown efficiency was tested (Fig. 8D). We did not show the protein level of ZC3H3 in knockdown cells because antibody against ZC3H3 was unavailable. To exclude the possibility that the upregulation or downregulation of ZC3H3 was cytotoxic to DF-1 cells, we examined the viability of the transfected DF-1 cells and found that no significant changes were observed (data not shown). As shown in Fig. 8B and C, overexpression of ZC3H3 could significantly reduce the IBV and H9N2 titers, while knockdown of ZC3H3 had the opposite effect (Fig. 8E and F). Thus, we concluded that ZC3H3 also plays a role in regulating H9N2 and even IBV infections.

4. Discussion

Host factors that determine the virus course have always been of interest to scientists, as these factors are involved in the complicated process of host-virus interaction and may provide potential targets for antiviral treatment. In this study, we found 927 differentially expressed proteins in response to H9N2 virus infection. GO analysis showed that these proteins are involved in many cellular processes, including the biological process, metabolic process, binding, and catalytic activity. KEGG analysis showed that these proteins exert their effects mainly through glutathione metabolism, cell adhesion molecules, and adherens junction. Among the top 20 upregulated proteins, several proteins were involved in the innate immune response, one of which was ZCCHC3, that was found to play an antiviral role in H9N2 infection, and even IBV

Table 1
The upregulated proteins ranking in the top 20.

Name	Localization	Coverage (%)	Description
AURKA	Cytoplasm	39.7	Aurora kinase A
FOSL1	Nucleus	16.2	FOS like 1, AP-1 transcription factor subunit
IFI16	Nucleus	19.5	Gamma-interferon-inducible protein 16
ISG15	Nucleus	37	ISG15 ubiquitin like modifier
IFIT1	Cytoplasm	45.8	Interferon-induced protein with tetratricopeptide repeats 1
SAMD9	Nucleus	13.5	Sterile alpha motif domain-containing protein 9
RANBP6	Cytoplasm	9.6	Ran-binding protein 6
UBE2S	Cytoplasm	52.7	Ubiquitin-conjugating enzyme E2 S
UBE2C	Cytoplasm	51.4	Ubiquitin-conjugating enzyme E2 C
ZCCHC3	Cytoplasm, nucleus	32	Zinc finger CCHC domain-containing protein 3
HERC5	Nucleus	11.2	E3 ISG15–protein ligase HERC5
SOWAHC	Nucleus	22.7	Ankyrin repeat domain-containing protein SOWAHC
PCLAF	Mitochondria	45.9	PCNA-associated factor
GPX1	Extracellular	43.3	Glutathione peroxidase 1
H2AX	Nucleus	43.4	Histone H2AX
TNFRSF10A	Plasma membrane	13.9	Tumor necrosis factor receptor superfamily member 10A
PLEKHF2	Extracellular	36.9	Pleckstrin homology domain-containing family F member 2
PIP5K1A	Nucleus	20.3	Phosphatidylinositol 4-phosphate 5-kinase type-1 alpha
NT5C3A	Mitochondria	24.1	5′-nucleotidase, cytosolic IIIA
FTL	Cytoplasm	43.4	Ferritin light chain

Table 2
The downregulated proteins ranking in the top 20.

| Name	Localization	Coverage (%)	Description
CYP24A1	Mitochondria	42.6	cytochrome P450 family 24 subfamily A member 1
PDCD4	Nucleus	24.1	Programmed cell death protein 4
RICTOR	Nucleus	10.8	Rapamycin-insensitive companion of mTOR
SUSD2	Extracellular	28.6	Sushi domain-containing protein 2
ERBIN	Mitochondria	20.8	Erbb2 interacting protein
SYNM	Nucleus	22.8	Synemin
HECTD1	Nucleus	12.8	HECT domain E3 ubiquitin protein ligase 1
DHCR24	ER	21.1	Delta (24)-sterol reductase
FDFT1	Cytoplasm	51.6	Farnesyl-diphosphate farnesyltransferase 1
PLD1	Nucleus	14	Phospholipase D1
ALDH3B1	Cytoplasm	39.5	Aldehyde dehydrogenase family 3 member B1
PTGFRN	Extracellular	15.7	Prostaglandin F2 receptor negative regulator
TRIM24	Nucleus	16.3	Tripartite motif containing 24
UHRF1	Nucleus	32.8	Ubiquitin like with PHD and ring finger domains 1
P4HA2	Extracellular	26.9	Prolyl 4-hydroxylase subunit alpha-2
C8orf33	Nucleus	21.8	Chromosome 8 open reading frame 33
BCAM	Extracellular	27.2	Basal cell adhesion molecule
CPLX2	Nucleus	48.5	Complexin-2
KANK2	Nucleus	26.9	KN motif and ankyrin repeat domain-containing protein 2
LIMCH1	Nucleus	18.4	LIM and calponin homology domains-containing protein 1

infection.

Back in 2008, Liu et.al for the first time reported the cellular proteomic response to avian H9N2 virus infection in AGS cells and identified many differentially expressed proteins, including cytokeratin, prohibitin, chloride intracellular channel protein 1, and nucleoside diphosphate kinase A (Liu et al., 2008). However, they did not address the underlying mechanisms by which these proteins functioned on this virus. Sun et.al identified that the spliceosome could be the main pathway that affected NP expression and H7N9 replication (Sun et al., 2015). Most recently, the mitochondrial-related proteins, including ATP synthase, H+ transporting, mitochondrial Fo complex subunit B1 (ATP5F1) and enoyl-CoA hydratase (ECHS1) were found to be differentially expressed during H5N1 and H9N2 infections (Yang et al., 2021). Although numerous proteomic studies in regard to AIV infections were done, the effects and the underlying mechanisms of these differentially expressed proteins have been rarely addressed. Thus, it is a pressing need to elaborate on how they function on virus infections.

Our proteomic results showed that ZCCHC3 expression could be upregulated by H9N2 infection, which is not consistent with the PRV infection, as it markedly reduced ZCCHC3 expression, although ZCCHC3 has antiviral effects on both viruses (Chen et al., 2022). It is well-know that transcription factors regulate protein activity. For example, early growth response gene 1 (EGR1) is a transcription factor that regulates IFN-regulated antiviral (IRAV) protein to inhibit porcine epidemic diarrhea virus (PEDV) virus infection (Wang et al., 2021). We speculated that there are the transcription factors that could upregulate ZCCHC3 protein to help host cells defend against virus invasion. PRV has the ability to manipulate the host machinery to decrease ZCCHC3 expression in response to infection, while H9N2 virus cannot reduce ZCCHC3 expression, in spite of the ability to antagonize ZCCHC3 by NS1. This indicates that other host factors may play a role in counteracting NS1. Upon SeV stimulation, ZCCHC3 bound with RIG-I and viral RNA promotes RIG-I to bind with viral RNA. In the meanwhile, ZCCHC3 activates RIG-I by promoting K63-linked ubiquitination of RIG-I through tripartite motif protein 25 (TRIM25) (Lian et al., 2018b). However, whether ZCCHC3 detects IAV RNA and how it responds to trigger IFN signaling needs to be further explored, as previous studies mainly focus on SeV infection, although IAV and SeV share some similarities.

IAVs are known to have developed multiple strategies to evade the host immunity. NS1 is one of the known factors that antagonize host innate immune responses (Chen et al., 2018). For example, NS1 inhibits the activation of RIG-I by suppressing its ubiquitination (Guo et al., 2007; Mibayashi et al., 2007). In addition, it also inhibits the expression of protein kinase R (PKR) and IFNs, thereby aiding in IAV replication (Min et al., 2007). Given the ability of NS1 to antagonize innate signaling, we raised the possibility that NS1 could block the ZCCHC3-mediated IFN signaling. As expected, the results showed that NS1 could attenuate the antiviral effect of ZCCHC3 on H9N2 virus. However, we did not know how NS1 functioned in this process. One possible reason is that NS1 could directly inhibit ZCCHC3 protein level, through degrading it by the proteasomal or lysosomal pathway. The other reason is that NS1 may inhibit the phosphorylation of interferon regulating factor 3 (IRF3) or IRF7, block the activation of nuclear factor-κB (NF-κB), or suppress the dimerization of signal transducer and activator of transcription1 (STAT1) and STAT2 during anti-H9N2 activity mediated by ZCCHC3. Additionally, NS1 may block polyadenylation of ZCCHC3 mRNA, thus attenuating the antiviral effect. These hypotheses deserve further investigation.

In conclusion, we presented a distinct cellular proteomic response to H9N2 infection and confirmed the critical role of ZCCHC3 in antiviral activity. ZCCHC3 was markedly induced by H9N2 infection and was found to exert inhibitory effects on H9N2 infection. Mechanistically, ZCCHC3 increased the expression of IFN-β and other antiviral genes, thus inhibiting viral replication. Importantly, NS1 protein showed a suppressive effect on ZCCHC3-mediated antiviral activity. Finally, chicken ZC3H3 could also suppress the growth of H9N2, and even IBV. Collectively, these data reveal a novel role of ZCCHC3 against H9N2 infection , contributing to the knowledge of virus-host interactions.

A

A549 cells

B

A549 cells

C

HEK293T cells

D

HEK293T cells
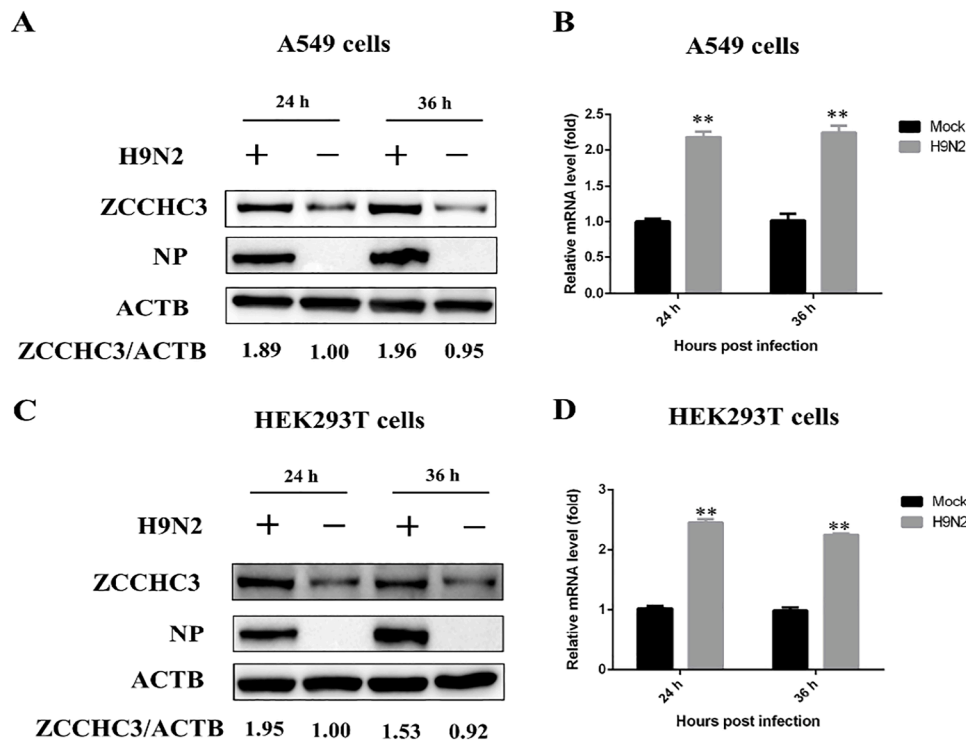
Fig. 3. Endogenous ZCCHC3 is induced by H9N2 infection. (A and B) A549 cells were infected with H9N2 virus (MOI=1) or mock-infected. After 24 h or 36 h, cells were collected for the detection of the protein levels and the mRNA levels, as indicated. (C and D) HEK293T cells were infected with H9N2 virus (MOI=1) or mock-infected for 24 h or 36 h. Then, cells were harvested and detected for the protein level and the mRNA levels, as indicated. Data are exhibited as mean $\pm$ SD. ** $p < 0.01$, p < 0.05.

A

B

C

D
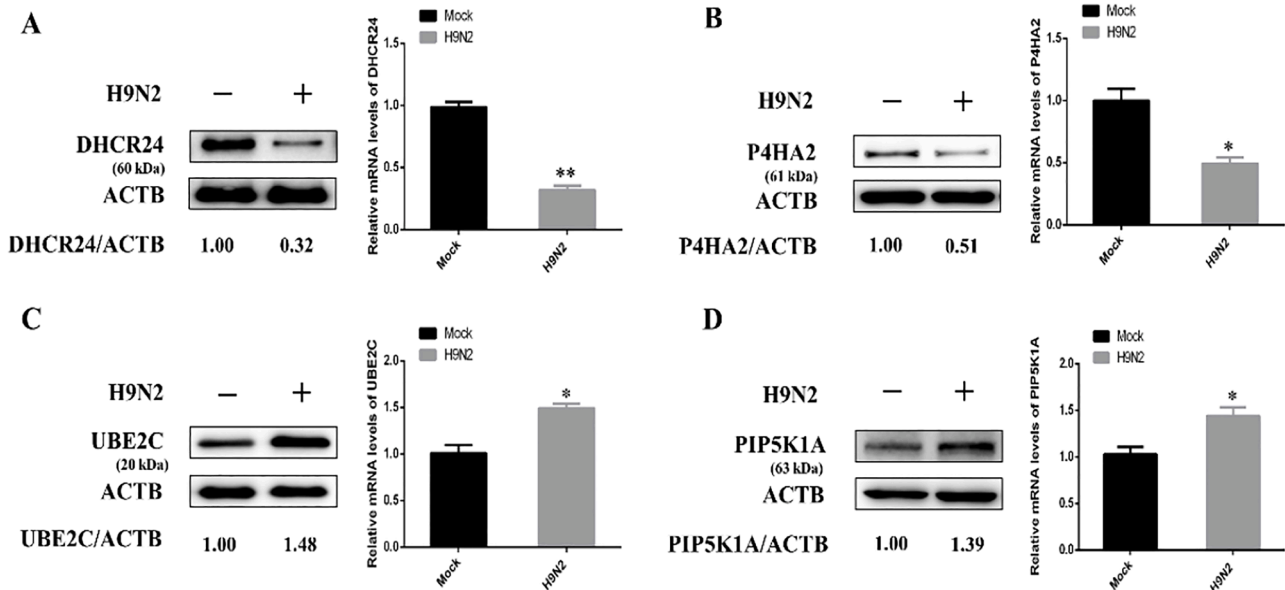
Fig. 4. Validation of other factors in A549 cells during viral infection. The samples were the same from Fig 3A and B at 24 h. (A, B, C, and D) The protein levels and mRNA levels of DHCR24, P4HA2, UBE2C, and PIP5K1A were detected by western blotting and real-time PCR. Data are exhibited as mean $\pm$ SD. ** $p < 0.01$, p < 0.05.

Author statement

YXC and YZ conceived and designed experiment. YXC and YSW performed the experiments. YXC, WZL, GZT, and YKC analyzed the data. YXC wrote and revised the paper. All authors contributed to this paper and approved the final manuscript.

### Declaration of Competing Interest

The authors declare no conflicts of interest that could have appeared to affect the work in this paper.
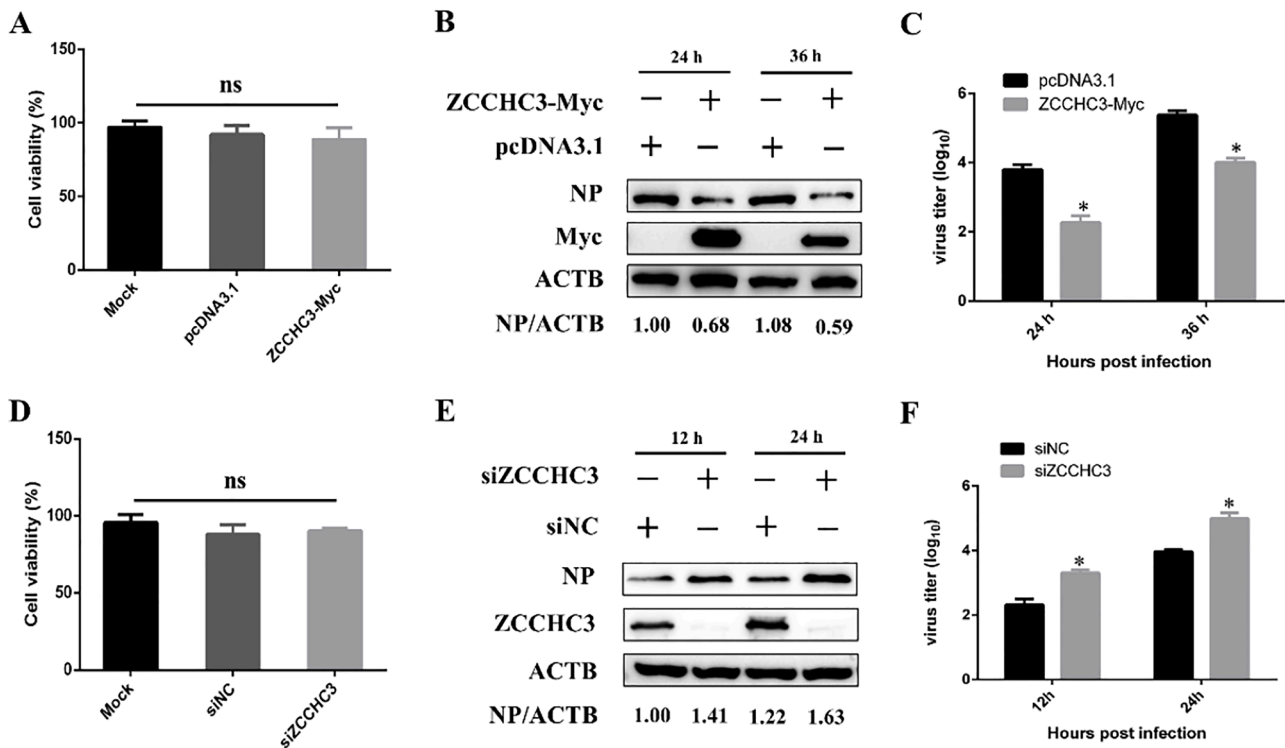
Fig. 5. Antiviral effect of ZCCHC3 on H9N2 virus in A549 cells. (A) A549 cells were transfected with the indicated plasmids for 36 h. The cells were collected and their viability was assessed by the amount. (B) A549 cells were transfected with the plasmids expressing ZCCHC3-Myc (2 μg) or pcDNA3.1 (2 μg) for 24 h. Cells were then infected with H9N2 virus (MOI=1) and harvested at the indicated time points for the analysis of the indicated protein levels. (C) The supernatant was collected from (B) and the virus titer was calculated by TCID$_{50}$ assay. (D) A549 cells were transfected with the indicated siRNA and the cell viability was assessed. (E) A549 cells were transfected with siNC or siZCCHC3 for 24 h and infected by H9N2 virus (MOI=1). The cells were collected and examined for the indicated protein levels. (F) The supernatant was harvested from (E) and H9N2 virus titer was measured by TCID$_{50}$ assay. Data are exhibited as mean ± SD. ** $p < 0.01$, $p < 0.05$.
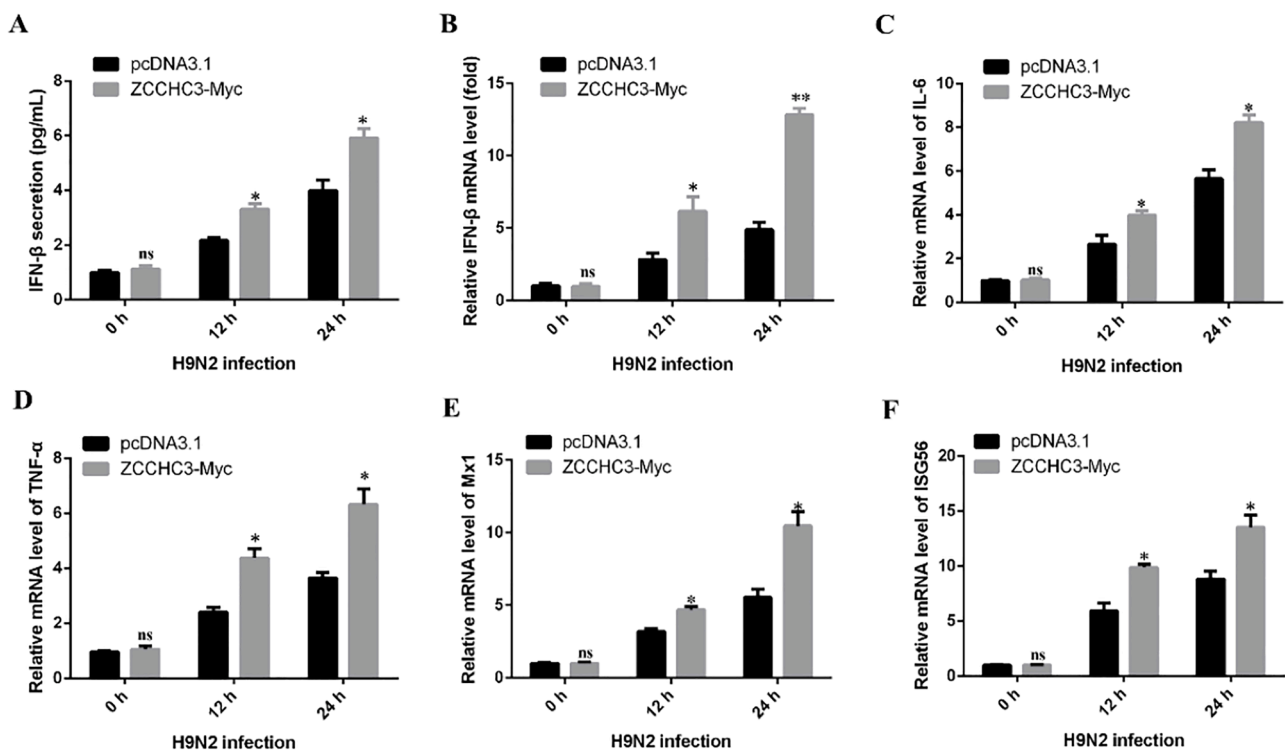
Fig. 6. ZCCHC3 promotes IFN-β expression. A549 cells were transfected with the plasmids expressing ZCCHC3-Myc (2 μg) or pcDNA3.1 (2 μg) for 24 h and infected with H9N2 virus (MOI=1). At the indicated time points, the supernatant and cells were collected. (A) The secretion of IFN-β was measured by ELISA. (B, C, D, E, and F) The mRNA levels of IFN-β, IL-6, TNF-α, Mx1, and ISG56 were examined using real-time PCR. Data are exhibited as mean ± SD. ** $p < 0.01$, $p < 0.05$.
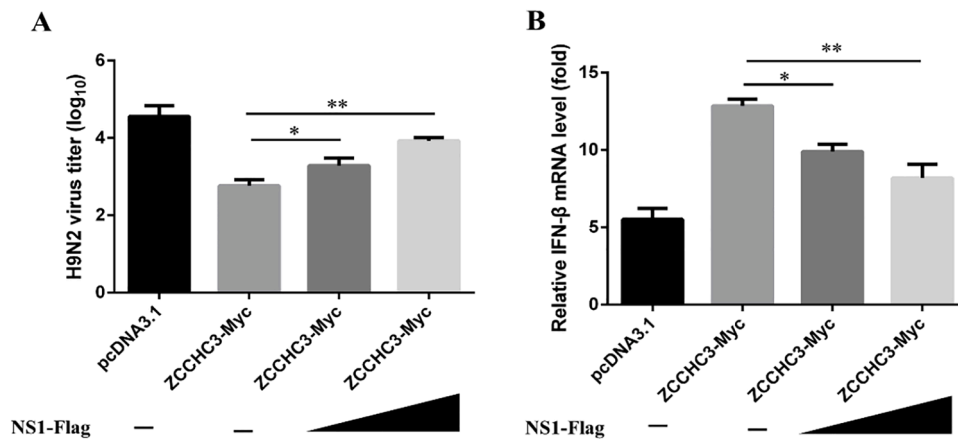
Fig. 7. NS1 attenuates the antiviral effect of ZCCHC3 by downregulating IFN-β. (A) A549 cells were transfected with the indicated plasmids for 24 h and then infected by H9N2 virus (MOI=1) for 24 h. The culture supernatant was collected and the virus titer was measured by TCID$_{50}$ assay. (B) The total RNA was extracted from (A) and the mRNA level of IFN-β was measured by real-time PCR. Data are exhibited as mean ± SD. ** p < 0.01, p < 0.05.
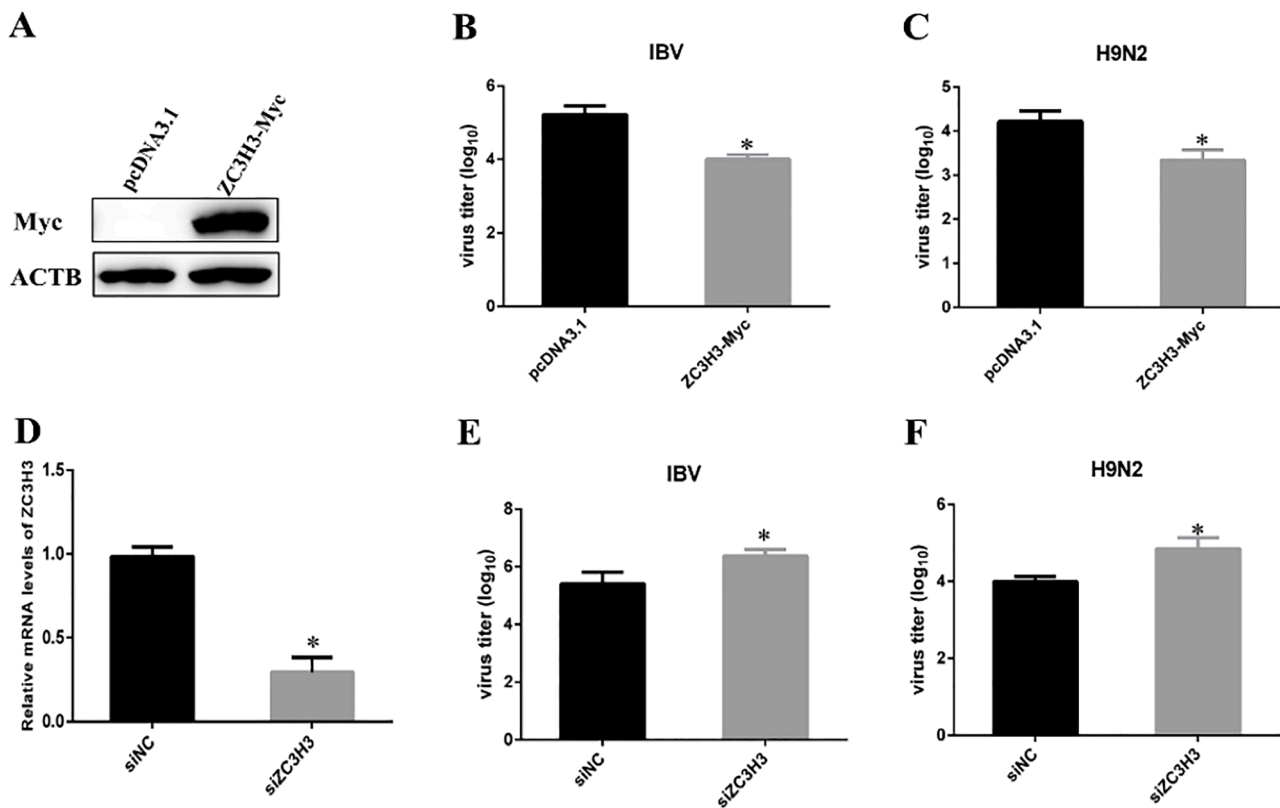
Fig. 8. Chicken zinc finger CCCH-type containing 3 (ZC3H3) inhibits the growth of H9N2 and IBV. (A) The protein level of ZC3H3-Myc was examined in DF-1 cells transfected with expressing-ZC3H3-Myc plasmids. (B, C) DF-1 cells were transfected with the ZC3H3-Myc plasmids or the pcDNA3.1 for 24 h. Cells were then infected with IBV (MOI=0.1) or H9N2 virus (MOI=1) for 24 h and the culture supernatant was collected and analyzed by TCID$_{50}$ assay for the virus titers. (D) DF-1 cells were transfected with the siZC3H3 or siNC for 24 h. The mRNA level of ZC3H3 was determined by real-time PCR. (E, F) DF-1 cells were transfected with the indicated siRNA for 24 h. Cells were then infected with IBV (MOI=0.1) or H9N2 virus (MOI=1). The virus titers were measured by TCID$_{50}$ assay from the culture supernatant. Data are exhibited as mean ± SD. ** p < 0.01, p < 0.05.

Supplementary materials

Supplementary material associated with this article can be found, in the online version, at doi:10.1016/j.virusres.2022.198876.

References

Bouvier, N.M., Palese, P., 2008. The biology of influenza viruses. Vaccine 26. https://doi.org/10.1016/j.vaccine.2008.07.039.

Bui, C.M., Adam, D.C., Njoto, E., Scotch, M., MacIntyre, C.R., 2018. Characterising routes of H5N1 and H7N9 spread in China using Bayesian phylogeographical analysis. Emerg. Microbes Infect. 7. https://doi.org/10.1038/s41426-018-0185-z.

Chen, X., Kong, N., Xu, J., Wang, J., Zhang, M., Ruan, K., Li, L., Zhang, Y., Zheng, H., Tong, W., Li, G., Shan, T., Tong, G., 2021. Pseudorabies virus UL24 antagonizes OASL-mediated antiviral effect. Virus Res. 295, 198276 https://doi.org/10.1016/j.virusres.2020.198276.

Chen, X., Liu, S., Goraya, M.U., Maarouf, M., Huang, S., Chen, J.L., 2018. Host immune response to influenza A virus infection. Front. Immunol. https://doi.org/10.3389/fimmu.2018.00320.

Chen, X., Shan, T., Sun, D., Zhai, H., Dong, S., Kong, N., Zheng, H., Tong, W., Tong, G., 2022. Host Zinc-finger CCHC-type containing protein 3 inhibits pseudorabies virus proliferation by regulating type I interferon signaling. Gene 827. https://doi.org/10.1016/j.gene.2022.146480.

Contreras, X., Salifou, K., Sanchez, G., Helsmoortel, M., Beyne, E., Bluy, L., Pelletier, S., Rousset, E., Rouquier, S., Kiernan, R., 2018. Nuclear RNA surveillance complexes silence HIV-1 transcription. PLoS Pathog. 14 https://doi.org/10.1371/journal.ppat.1006950.

Fatima, U., Zhang, Z., Zhang, H., Wang, X.F., Xu, L., Chu, X., Ji, S., Wang, X., 2019. Equine Mx1 restricts influenza a virus replication by targeting at distinct site of its nucleoprotein. Viruses 11. https://doi.org/10.3390/v11121114.

Gu, M., Xu, L., Wang, X., Liu, X., 2017. Current situation of H9N2 subtype avian influenza in China. Vet. Res. https://doi.org/10.1186/s13567-017-0453-2.

Guan, Y., Smith, G.J.D., 2013. The emergence and diversification of panzootic H5N1 influenza viruses. Virus Res. 178, 35–43. https://doi.org/10.1016/j.virusres.2013.05.012.

Guo, Z., Chen, L.M., Zeng, H., Gomez, J.A., Plowden, J., Fujita, T., Katz, J.M., Donis, R.O., Sambhara, S., 2007. NS1 protein of influenza A virus inhibits the function of intracytoplasmic pathogen sensor, RIG-I. Am. J. Respir. Cell Mol. Biol. 36, 263–269. https://doi.org/10.1165/rcmb.2006-0283RC.

Huang, H., Xu, H., Li, P., Ye, X., Chen, W., Chen, W., Huang, X., 2021. Zinc finger C3H1 domain-containing protein (ZFC3H1) evaluates the prognosis and treatment of prostate adenocarcinoma (PRAD): A study based on TCGA data. Bioengineered 12, 5504–5515. https://doi.org/10.1080/21655979.2021.1965442.

Lian, H., Wei, J., Zang, R., Ye, W., Yang, Q., Zhang, X.N., Chen, Y.da, Fu, Y.Z., Hu, M.M., Lei, C.Q., Luo, W.W., Li, S., Shu, H.B., 2018a. ZCCHC3 is a co-sensor of cGAS for dsDNA recognition in innate immune response. Nat. Commun. 9 https://doi.org/10.1038/s41467-018-05559-w.

Lian, H., Zang, R., Wei, J., Ye, W., Hu, M.M., Chen, Y.da, Zhang, X.N., Guo, Y., Lei, C.Q., Yang, Q., Luo, W.W., Li, S., Shu, H.B., 2018b. The Zinc-Finger Protein ZCCHC3 Binds RNA and Facilitates Viral RNA Sensing and Activation of the RIG-I-like Receptors. Immunity 49, 438–448. https://doi.org/10.1016/j.immuni.2018.08.014 e5.

Lin, R.J., Chien, H.L., Lin, S.Y., Chang, B.L., Yu, H.P., Tang, W.C., Lin, Y.L., 2013. MCPIP1 ribonuclease exhibits broad-spectrum antiviral effects through viral RNA binding and degradation. Nucleic Acids Res. 41, 3314–3326. https://doi.org/10.1093/nar/gkt019.

Liu, N., Song, W., Wang, P., Lee, K., Chan, W., Chen, H., Cai, Z., 2008. Proteomics analysis of differential expression of cellular proteins in response to avian H9N2 virus infection in human cells. Proteomics 8, 1851–1858. https://doi.org/10.1002/pmic.200700757.

Long, J.S., Mistry, B., Haslam, S.M., Barclay, W.S., 2019. Host and viral determinants of influenza A virus species specificity. Nat. Rev. Microbiol. https://doi.org/10.1038/s41579-018-0115-z.

Mibayashi, M., Martínez-Sobrido, L., Loo, Y.-M., Cárdenas, W.B., Gale, M., García-Sastre, A., 2007. Inhibition of retinoic acid-inducible gene I-Mediated Induction of Beta Interferon by the NS1 Protein of Influenza A Virus. J. Virol. 81, 514–524.

Min, J.Y., Li, S., Sen, G.C., Krug, R.M., 2007. A site on the influenza A virus NS1 protein mediates both inhibition of PKR activation and temporal regulation of viral RNA synthesis. Virology 363, 236–243. https://doi.org/10.1016/j.virol.2007.01.038.

Poovorawan, Y., Pyungporn, S., Prachayangprecha, S., Makkoch, J., 2013. Global alert to avian influenza virus infection: From H5N1 to H7N9. Pathogens and Global Health. https://doi.org/10.1179/2047773213Y.0000000103.

Qu, H., Li, J., Yang, L., Sun, L., Liu, W., He, H., 2016. Influenza A Virus-induced expression of ISG20 inhibits viral replication by interacting with nucleoprotein. Virus Genes 52, 759–767. https://doi.org/10.1007/s11262-016-1366-2.

Sullivan, S.J., Jacobson, R.M., Dowdle, W.R., Poland, G.A., 2010. 2009 H1N1 influenza. Mayo Clin. Proc. https://doi.org/10.4065/mcp.2009.0588.

Sun, N., Sun, W., Li, S., Yang, J., Yang, L., Quan, G., Gao, X., Wang, Z., Cheng, X., Li, Z., Peng, Q., Liu, N., 2015. Proteomics analysis of cellular proteins co-immunoprecipitated with nucleoprotein of influenza a virus (H7N9). Int. J. Mol. Sci. 16, 25982–25998. https://doi.org/10.3390/ijms161125934.

Tong, S., Zhu, X., Li, Y., Shi, M., Zhang, J., Bourgeois, M., Yang, H., Chen, X., Recuenco, S., Gomez, J., Chen, L.M., Johnson, A., Tao, Y., Dreyfus, C., Yu, W., McBride, R., Carney, P.J., Gilbert, A.T., Chang, J., Guo, Z., Davis, C.T., Paulson, J.C., Stevens, J., Rupprecht, C.E., Holmes, E.C., Wilson, I.A., Donis, R.O., 2013. New world bats harbor diverse influenza A viruses. PLoS Pathog. 9 https://doi.org/10.1371/journal.ppat.1003657.

Trilla, A., Trilla, G., Daer, C., 2008. The 1918 "Spanish Flu" in Spain. Clin. Infect. Dis. https://doi.org/10.1086/590567.

Wang, H., Kong, N., Jiao, Y., Dong, S., Sun, D., Chen, X., Zheng, H., Tong, W., Yu, H., Yu, L., Zhang, W., Tong, G., Shan, T., 2021. EGR1 Suppresses Porcine Epidemic Diarrhea Virus Replication by Regulating IRAV To Degrade Viral Nucleocapsid Protein.

Watanabe, T., Watanabe, S., Kawaoka, Y., 2010. Cellular networks involved in the influenza virus life cycle. Cell Host Microbe. https://doi.org/10.1016/j.chom.2010.05.008.

Wu, X., Xiao, L., Li, L., 2020. Research progress on human infection with avian influenza H7N9. Front. Med. https://doi.org/10.1007/s11684-020-0739-z.

Wu, Ying, Wu, Yan, Tefsen, B., Shi, Y., Gao, G.F., 2014. Bat-derived influenza-like viruses H17N10 and H18N11. Trends Microbiol. https://doi.org/10.1016/j.tim.2014.01.010.

Yang, Y., Zhang, Y., Yang, C., Fang, F., Wang, Y., Chang, H., Chen, Z., Chen, P., 2021. Differential mitochondrial proteomic analysis of A549 cells infected with avian influenza virus subtypes H5 and H9. Virol. J. 18 https://doi.org/10.1186/s12985-021-01512-4.

Zhang, B., Goraya, M.U., Chen, N., Xu, L., Hong, Y., Zhu, M., Chen, J.L., 2020. Zinc finger CCCH-Type antiviral protein 1 restricts the viral replication by positively regulating type I interferon response. Front. Microbiol. 11 https://doi.org/10.3389/fmicb.2020.01912.